HHS Public Access

Author manuscript

J Nutr Biochem. Author manuscript; available in PMC 2021 May 26.

Published in final edited form as:

J Nutr Biochem. 2016 August ; 34: 118–125. doi:10.1016/j.jnutbio.2016.05.003.

MICRORNA -19A/B MEDIATE GRAPE SEED PROCYANIDIN EXTRACT INDUCED ANTINEOPLASTIC EFFECTS AGAINST LUNG CANCER

Jenny T. Mao[1], **Bingye Xue**[1], **Jane Smoake**[1], **Qing-Yi Lu**[2], **Heesung Park**[1], **Susanne M. Henning**[2], **Windie Burns**[3], **Alvise Bernabei**[4], **David Elashoff**[5], **Kenneth J. Serio**[6], **Larry Massie**[3]

[1]Pulmonary, Critical Care, and Sleep Section, New Mexico Veterans Administration Health Care System, University of New Mexico.

[2]UCLA Center for Human Nutrition, David Geffen School of Medicine at UCLA.

[3]Pathology and Clinical Laboratory Services. New Mexico Veterans Administration Health Care System, University of New Mexico.

[4]Cardiothoracic Surgery Section, New Mexico Veterans Administration Health Care System, University of New Mexico.

[5]Department of Biostatistics, Department of Medicine, David Geffen School of Medicine at UCLA.

[6]Pulmonary & Critical Care Medicine, Scripps Green Hospital.

Abstract

Oncomirs are microRNAs (miRNA) associated with carcinogenesis and malignant transformation. They have emerged as potential molecular targets for anti-cancer therapy. We hypothesize that grape seed procyanidin extract (GSE) exerts antineoplastic effects through modulations of oncomirs and their downstream targets. We found that GSE significantly down-regulated oncomirs miR-19a and −19b in a variety of lung neoplastic cells. GSE also increased mRNA and protein levels of insulin-like growth factor II receptor (IGF-2R) and phosphatase and tensin homolog (PTEN), both predicted targets of miR-19a and −19b. Furthermore, GSE significantly increased PTEN activity and decreased AKT phosphorylation in A549 cells. Transfection of miR-19a and −19b mimics reversed the up-regulations of *IGF2R* and *PTEN* gene expression and abrogated the GSE induced anti-proliferative response. Additionally, oral administration of leucoselect phytosome, comprised of standardized grape seed oligomeric procyanidins complexed with soy phospholipids, to athymic nude mice via gavage, significantly down-regulated miR-19a, −19b and the miR-17–92 cluster host gene (MIR17HG) expressions, increased IGF-2R, PTEN, decreased phosphorylated-AKT in A549 xenograft tumors, and markedly inhibited tumor growth. To confirm

Address Correspondence to: Jenny T. Mao, M.D., Pulmonary, Critical Care, & Sleep Section, New Mexico VA Health Care System, 1501 San Pedro Drive. SE, Albuquerque, New Mexico, Phone: (505) 265-1711, ext 4509; FAX: (505) 256-5751, jenny.mao@va.gov.

The authors have no conflict of interest to disclose.

the absorption of orally administered GSE, plasma procyanidin B1 levels, between 60–90 minutes after gavage of leucoselect phytosome (400 mg/kg), were measured by LC/MS at week 2 and 8 of treatment; the estimated concentration that was associated with 50% growth inhibition (IC_{50}) (1.3 μg/ml) *in vitro* was much higher than the IC_{50} (0.032–0.13μg/ml) observed *in vivo*. Our findings reveal novel antineoplastic mechanisms by GSE and support the clinical translation of leucoselect phytosome as an anti-neoplastic and chemopreventive agent for lung cancer.

Keywords

MiRNA; IGF-2R; PTEN; AKT; Grape seed procyanidin B1 bioavailability

INTRODUCTION

Derived from seeds of grapes (*Vitis vinifera)*, GSE is high in polyphenolic bioflavonoids including proanthocyanidins [1]. Proanthocyanidins have been shown to have antioxidant capabilities 20 and 50 times that of vitamin C and E, respectively [2]. Widely available as a health food supplement, GSE is used to improve cardiovascular health [3]. Preclinical studies have shown antineoplastic effects of GSE against a variety of cancers, including non-small cell lung cancer (NSCLC) [4–7]. However, the molecular mechanisms responsible for the antineoplastic properties of GSE are incompletely understood, and little is known about the effects of GSE on microRNA (miRNA) expression in lung cancer. MiRNAs are small noncoding RNA molecules with regulatory function and tissue specificity that can modulate multiple molecular targets across several mechanistic pathways. MiRNAs function as epigenetic modifiers and mediate post-transcriptional regulation of specific mRNAs, mainly through mRNA degradation and/or translational repression [8]. Various miRNAs have been identified as oncomirs, based on their associations with cancer [9]. Oncomirs can mediate pro- or anti-tumor effects, are stable against degradation, and can be easily quantified in tissue samples and body fluids with simple assays like real time (q)PCR. Ample studies have shown that specific miRNA signatures in biospecimens had remarkable sensitivity and specificity in discriminating cancer patients from healthy subjects [10, 11]. These characteristics support the potential of oncomirs as therapeutic targets and surrogate endpoint biomarkers (SEBM) for lung cancer treatment and chemoprevention. We therefore hypothesize that GSE is capable of exerting its antineoplastic effects through modulations of oncomirs.

We delineated the roles of miR-19a/b, and their targets, IGF-2R and PTEN, in mediating the anti-neoplastic properties of GSE against lung cancer. We further demonstrated the *in vivo* anticancer efficacy of leucoselect phytosome, a standardized GSE, in nude mice, which correlated with the *in vitro* findings. In addition, plasma procyandin B1 levels measured after oral gavage confirmed bioavailability of leucoselect phytosome in nude mice. Our findings reveal novel anti-neoplastic mechanisms by GSE and support the further investigation of leucoselect phytosome as an anti-neoplastic and chemopreventive agent for lung cancer.

MATERIALS AND METHODS

Cell Culture:

As models to evaluate the anti-neoplastic effect of GSE against lung cancer, the human NSCLC lines, A549, H520, H1299, BEAS-2B (ATCC; Manassas, VA), and the bronchial premalignant cell line 1198 generously provided by Dr. Klein-Santos (Fox Chase Cancer Center, Philadelphia, PA) [12], were studied *in vitro*. Experiments involving all commercial cell lines were initiated within 6 months of purchase. Cell lines were not further authenticated. ATCC uses Short Tandem Repeat profiling for cell line authentication. Cells were maintained as monolayers in an atmosphere of 5% CO_2 in air at 37°C in 25-cm^2 tissue culture flasks containing 5.0 ml of RPMI-1640 medium supplemented with 10% FBS, 100 units/ml of penicillin, 0.1 mg/ml of streptomycin, and 2 mM of glutamine (JRH Biosciences; Lenexa, KS) for A549; and RPMI-1640 medium with 2 mM L-glutamine adjusted to contain 1.5 g/L sodium bicarbonate, 4.5 g/L glucose, 10 mM HEPES, and 1.0 mM sodium pyruvate, 90%; fetal bovine serum, 10% for H1299 and H520 cells. Aliquots of 0.1×10^6 A549 or H520 cells were incubated at 37°C for 2 h. Varying doses of GSE (6, 12, 15, 30, 45, and 60 μg/ml) were added and the cells were incubated at 37°C for 18–44 h. The dose range of GSE was chosen based on considerations from prior published studies [6, 7]. Primary normal human bronchial epithelial (NHBE) cells (Cambrex, Walkersville, MD) and BEAS-2B cells (non-tumorigenic bronchial epithelial cells) were used as control. NHBE cells were maintained according to the manufacturer's instructions. Aliquots of 0.5×10^6 of NHBE and BEAS-2B cells were plated in wells and incubated at 37°C for 18–44h. For MTT assays, cells were plated at concentration of $6–8 \times 10^3$ cells/well in 96 well plates, conditioned and cultured for 18–44 h.

All conditioned culture supernatants and total RNA were harvested with cell lysates stored at −80°C until analysis, when applicable. Samples of mRNA were collected using the miRNeasy Mini Kit (Qiagen Inc, Valencia, CA), per the manufacturer's instructions.

GSE Preparations.

Standardized GSE (90% procyanidins, which were members of the proanthocyanidins class of flavonoids), was purchased from Organic Herb Inc., China. Stock solutions of GSE were made by dissolving the extract with deionized water. Aliquots of the stock were stored at −80°C and used only once for each set of experiments. For oral gavage, suspensions of varying doses of Leucoselect Phytosome (Indena Inc., Milan, Italy), comprised of standardized oligomeric procyanidins complexed with soy phospholipid (1:2.6 w/w), were freshly prepared daily in deionized water for each treatment group just prior to gavage.

Animals and Tumor Xenograft Assay.

Female athymic nude mice (8–9 weeks old) were used and purchased from the National Cancer Institute and provided the sterilized AIN76A diet and water *ad libitum*. All the mice were housed in the Vivarium of the New Mexico VA Health Care System and were maintained under the following conditions: 12-h dark/12-h light cycle, 24 ± 2°C temperature, and 50 ± 10% humidity. To determine the *in vivo* efficacy of GSE against human NSCLC tumor xenograft growth, exponentially growing A549 cells were mixed at a

1:1 ratio with Matrigel (Trevigen Inc. Gaithersburg, MD), and a 100 μL suspension containing 1.2×10^6 cells was injected subcutaneously in the right flank of each mouse. Mice were randomly divided into 4 treatment groups ($n = 9$ per group), and gavaged every morning with varying doses of leucoselect phytosome (0, 200, 300 and 400 mg/kg). Clinical scoring including body wt, signs of illness or suffering were assessed daily and tumor growth was regularly monitored. Tumor size was determined using the ellipsoid volume formula ($\pi/6 \times L \times W \times H$) [13]. The experiment was terminated at 56 days after tumor cell inoculation following the guidelines of Institutional Animal Care and Use Committee. Plasma and tumors were harvested at various time points for biomarker determination.

Cell Death ELISA

To quantify apoptosis in the conditioned cells, specific measurements of mono- and oligonucleosomes by immunochemical determination of histone-complexed DNA fragments in the cytoplasmic fraction of conditioned cell culture lysates were performed using the cell death ELISA kit according to the manufacturer's instructions (Roche; Indianapolis, IN) as previously described [14].

Quantification of Cell Proliferation - MTT Assay

To quantify cellular proliferation in conditioned cells, The MTT Cell Proliferation Assay (ATCC; Manassas, VA) was used according to the manufacturer's instructions.

Real Time (q) PCR for Quantification of miRNA and mRNA Expression

The total RNA isolated using miRNeasy Mini kit was converted to first strand cDNA via universal tailing and reverse transcription. The cDNA template was mixed with qPCR Master Mix and aliquoted into each well of the 96-well plate containing an array of pre-dispensed miRNA-specific primer sets (MAH-100, SA Bioscience; Fredrick, MD). QPCR was performed on the Bio-Rad MyiQ cycler (BioRad; Hercules, CA). Following identification of miRNA of interest, further validation using qPCR with specific miR-19a and −19b primers was performed, per manufacturer's instructions. The qPCR reactions for the miR-17–92 cluster host gene (MIR17HG), IGF2R and PTEN genes were performed using reagents, specific primers from SA Bioscience per the manufacturer's instructions. Any C_t greater than 35 was considered a negative call. The values were first normalized to beta-actin, then to control, using $\Delta\Delta C_t$ based fold-change calculations from raw threshold cycle (C_t) data. Data are depicted in fold changes normalized to control. Negative fold change represents down-regulation - a reduction of 50% or 75% from control (untreated cells) is equivalent to −2 or −3 fold changes, respectively.

MiRNA *in situ* Hybridization Assay

In situ hybridization (ISH) of miR-19a and −19b were performed using the QuantiGene® ViewRNA miRNA ISH cell assay kit (Affymetrix Panomics, Santa Clara, CA). Briefly, 8×10^3 cells/well were plated in a 96 well plate precoated with Poly-L-Lysine. After 2 h adherence, cells were conditioned with varying doses of GSE overnight, then fixed in 4% formaldehyde, cross linked with EDC, permeablized with detergent and digested with

protease and then hybridized to target probes, followed by amplification and detection steps as per manufacturer's instruction.

MiRNA Mimic Transfection

Transfections of mir-19a or miR-19b mimics into lung neoplastic cells were achieved using miRNA specific mimics, and transfecting reagents according to manufacturer's instructions (Qiagen Inc. (Valencia, CA). Briefly, 6–8 × 10^3 of cells in 150 μl medium were aliquoted into 96-well plates. After 1 h of adherence, 50 μl of specific miRNA transfection complexes were gently added to the cells with gentle swirling. The cells were incubated for 4 h, then conditioned overnight with GSE, followed by the MTT assay. Cell conditions were scaled up 10 fold in 12 well plates for total RNA harvest.

IGF-2R ELISA

An IGF2R-specific ELISA was used to quantify IGF2R protein in conditioned cell lysates and culture supernatants per the manufacturer's instructions (R & D Systems, Minneapolis, MN). IGF2R levels from each sample were referenced to the concentrations of total protein. Total protein levels were determined using the Pierce BCA Protein Assay kit per the manufacturer's instruction (ThermoFisher Scientific, Waltham, MA).

PTEN Immunoblot

Following 22 h conditioning with varying doses of GSE, cells were rinsed twice with cold PBS before lysis in buffer containing 1:100 dilution of protease inhibitor cocktail (Sigma-Aldrich, St. Louis, MO). Proteins were extracted by centrifugation and quantified using the Pierce BCA Protein Assay Kit. Thirty μg of protein samples were loaded into each slot of the slot blot apparatus (PR600, Hoefer Inc., Holliston, MA) containing a PVDF membrane (Immobilon transfer membrane, Millipore, Bellerica, MA). After vacuum drying, the membrane was wet with methanol and washed twice with double-distilled (DD) H_2O, blocked with Blocker/Diluent A and B from the WesternBreeze Chromogenic Western Blot Immunodetection Kit (Invitrogen, Carlsbad, CA) for 30 minutes per the manufacturer's instruction. Briefly, the membrane was incubated with PTEN (D4.3) XP™ rabbit primary monoclonal antibody (mAb, Cell Signaling, Beverly, MA) at 1:1000 dilution with Blocker/Diluent A and B for 1 hr. Blots were rinsed 4 times with Antibody Wash from the kit, incubated with the secondary Ab for 30 minutes. After washing the membrane was Incubated with the Chromogenic Substrate, digitally imaged with densitometry measured using image J (NIH. Bethesda, MD).

PTEN Activity ELISA

After 22 h conditioning with varying doses of GSE, The PTEN Activity ELISA was used to quantify the effects of GSE on phosphatase activity of PTEN by detection of the product, PIP_2, per the manufacturer's instructions (Echelon Biosciences Inc. Salt Lake City, UT). Briefly, conditioned cells were lysed in lysis buffer followed by immunoprecipitation. PTEN were then diluted in the PTEN reaction buffer and incubated using $PI(3,4,5)P_3$ as a substrate. After the PTEN reactions were complete, reaction products were added to the $PI(4,5)P_2$-coated microplate and a $PI(4,5)P_2$ detector protein was then added for competitive binding.

A peroxidase-linked secondary detector and colorimetric detection was used to detect PI(4,5)P2 detector binding to the plate. The colorimetric signal was inversely proportional to the amount of PI(4,5)P_2 produced by PTEN.

Phospho-AKT (p-AKT) ELISA

Following 24 h of incubation, cell lysates were harvested to determine the effects of GSE on levels of P-AKT, using the Human/Mouse/Rat Phospho-AKT (S473) Pan Specific DuoSet IC ELISA kit per the manufacturer's instruction (R & D Systems, Minneapolis, MN). This ELISA kit specifically measures AKT phosphorylated at Ser473.

Immunohistochemistry for IGF-2R, PTEN, and Phospho-AKT

Tumor xenografts sections (5 μM) were stained for immunohistochemistry (IHC) with a primary anti- IGF2R monoclonal rabbit IgG antibody (1:1500 dilution, EMD Millipore), anti-PTEN polyclonal rabbit IgG antibody (1:100 dilution, R & D Systems, Minneapolis, MN), or anti-phosphor-AKT polyclonal rabbit IgG antibody (1:40 dilution, R & D Systems) and a diaminobenzidine detection reaction as previously detailed [19]. Up to five high-magnification fields were examined. IHC Score was determined by consensus of two dedicated readers (LM and JM), using a semi-quantitative method to evaluate the intensity of staining with a 0–3 scoring system (0, below the level of detection; 3, intense staining). When the intensity of staining was heterogeneous, the percentage of cancer cells staining at each intensity level was assessed. The final IHC score for each protein in each tumor was generated based on a composite score of the percent of positive cells and intensity of staining. Negative controls using nonimmune sera showed no staining.

Measurement of plasma procyanidin B1

Procyanidins were extracted from mouse plasma (0.2 mL) by incubating samples with 0.3 mL of enzyme solution (1000 U β-glucuronidase with 40 U sulfatase activity in 0.5 M NaH_2PO_4 pH 5.0 containing 2% ascorbic acid) for 45 minutes at 37°C. Following incubation, samples were extracted three times with ethyl acetate/2% ascorbic acid. Combined ethyl acetate extracts were dried, and residue was resolublized in 100 μL 50% aqueous methanol prior to analysis using LC/MS. Briefly, separation was performed on a Surveyor HPLC system equipped with a diode array detector (Thermo Finnigan, San Jose, CA) using a Zorbax SB-C18 column (4.6×150 mm, 3.5 μm; Agilent, Santa Clara, CA). A binary mobile phase consisting of solvent systems A and B was used in gradient elution where A was 1% acetic acid (v/v) in ddH_2O and B was acetonitrile. Mobile phase flow rate was 0.75 mL/min with a T splitter to make 0.25 mL/min flow to MS. Initial conditions was set at 98:2 A:B with a linear gradient to 75:25 from 0 to 25 min, and to 60:40 from 25 to 32 min. Following separation the column effluent was introduced by negative mode electrospray ionization (ESI) into an LCQ Advantage Ion Trap Mass Spectrometer. ESI capillary voltage was −4.0 kV, capillary temperature was 275°C, sheath gas flow was set at 40, and the normalized collision energy was set at 45%. Spectroscopic (UV at 280 nm) and MS/MS data (577/425) was collected and analyzed using Xcalibur software (Thermo Finnigan). Concentration of plasma procyanidin B1 was determined by internal calibration and ethyl gallate was used as an internal standard.

Statistical Analysis

Data were expressed as the mean ± SD in all circumstances where mean values are compared. Data were analyzed by paired Student's *t* test and/or ANOVA. Batch analyses were performed for each comparison group to eliminate interassay variability. Differences are considered significant when $p < 0.05$.

RESULTS

GSE significantly down-regulated oncomir miR-19a, miR-19b, and miR-17–92 cluster host gene (MIR17HG) expression in lung neoplastic cells and tumor xenografts.

Specific qPCR demonstrate the dose-dependent, down-regulation of miR-19a and −19b in A549 (Fig. 1A), 1198 (Fig. 1B) and H1299 cells (data not shown) by GSE. Further confirmation was obtained with miR-19a and −19b specific ISH assay in A549 cells (Fig 1C). In addition, the down-regulation of miR-19a/b by GSE appears to be at the pri-miRNA level, as GSE also down-regulated the expression of their host gene, MIR17HG (Fig 1D). Oral gavage of leucoselect phytosome, to athymic nude mice decreased expression of miR-19a/b (Fig 1E) and *MIR17HG* (Fig 1F) in the xenograft tumors.

GSE induced anti-proliferative and apoptotic effects in lung neoplastic cells and inhibited tumor xenograft growth.

To ascertain the anti-neoplastic property of GSE, we evaluated the ability of GSE to induce apoptosis and reduce proliferation in A549, H1299 and 1198. GSE dose-dependently inhibited proliferation (Fig 2A) and induced apoptosis (Fig. 2B & 2C) in these lung neoplastic cells. This is the first time GSE has been shown to exert antineoplastic effects on premalignant bronchial epithelial cells. As expected, far lower concentration of GSE is required to exert the same degree of anti-neoplastic effects on premalignant cells. Interestingly, much higher dose of GSE is required to induce apoptosis in H1299 cells than other cell lines, while the anti-proliferative dose response in H1299 is similar to A549. Treatment with leucoselect phytosome also significantly inhibited A549 tumor xenograft growth (Fig. 2D).

Transfection with miR-19a or miR-19b mimics abrogated the anti-proliferative effects of GSE in lung neoplastic cells.

To confirm that GSE-induced anti-proliferative effects involved down-regulation of miR-19a/b, A549 cells were transfected with miR-19a and −19b mimics. These mimics significantly abrogated the anti-proliferative effects of GSE in A549 (Fig. 3A and B), H1299 (Fig. 3C and D), H520 (Fig. 3E and F), and 1198 cells (data not shown).

GSE increased mRNA expressions of *IGF2R,* IGF-2R protein production/secretion by A549 cells and in xenograft tumors.,

We then evaluated the effects of GSE treatment on predicted targets of miR-19a/b that are known to play a role in cell proliferation and apoptosis, including IGF-2R. IGF-2R is a secretory protein that functions to bind IGF-2 and facilitates its clearance, thereby preventing IGF-2 signaling. GSE significantly increased mRNA expressions of *IGF2R*,

which was partially abrogated by miR-19b mimics inA549 cells (Fig. 4A). The reduction of IGF-2R protein production/secretion (Fig. 4B and 4C) were also partially reversed by transfection of miR-19b mimics (Fig. D). IHC scoring of IGF-2R in xenograft tumors further confirmed the increase of IGF-2R by leucoselect phytosome *in vivo*. (Fig 4E).

GSE increased *PTEN* mRNA expression, PTEN protein production/activity, and decreased P-AKT in A549 cells.

The effects of GSE on PTEN, another important target of miR-19a/b, was also evaluated. GSE significantly up-regulated PTEN mRNA expression, which was abrogated by miR-19b mimics (Fig 5A). GSE increased PTEN protein production in conditioned A549 cell lysates (Fig. 5B), and PTEN activity as quantified by measuring the ability of conditioned cells to convert PIP_3 to PIP_2 in comparison to control cells (Fig. 5C, n=2). PTEN IHC scoring in xenograft tumors further confirmed the increase of PTEN by leucoselect phytosome *in vivo* (Fig. 5D). PTEN protein acts as a negative regulator of the PI3K/AKT signaling pathway through its ability to dephosphorylate PIP_3. Accordingly, Overnight treatment of A549 cells with GSE also dose-dependently decreased phosphorylation (activation) of AKT (Fig. 5E). P-AKT IHC scoring in xenograft tumors further confirms the reduction of P-AKT by leucoselect phytosome *in vivo* (Fig. 5F).

Plasma procyanidin B1 as a bioavailability marker for leucoselect phytosome.

Levels of procyandiin B1 were measured in mouse plasma obtained between 60–90 minutes after gavage of leucoselect phytosome at week 2 and 8 of treatment. The plasma concentrations of procyanidin B1 were found to be 32.4 and 130 ng/ml, respectively (Table 1). Plasma procyanidin B1 appeared to increase with continued dosing.

DISCUSSION

In this study, we report for the first time, that GSE significantly and dose-dependently down-regulated the expression of well-known oncomirs, miR-19a and −19b [15], in lung neoplastic cells. Reduction of these oncomirs correlated with decreased cell proliferation and induction of apoptosis, as well as up-regulations of IGF2R and PTEN mRNA expressions, and their respective protein products. Both PTEN and IGF2R are predicted targets of miR-19a/b (TargetScanHuman, http://www.targetscan.org/vert_61). GSE also increased PTEN activity and decreased phosphorylation of AKT - a key procarcinogenic driver in lung cancer. Transfection with miR-19a or −19b mimics significantly abrogated the GSE-induced up-regulation of IGF2R and PTEN mRNA expression in A549 cells and reversed the anti-proliferative effects of GSE in A549 (adenocarcinoma), H520 (squamous cell carcinoma), H1299 (metastatic NSCLC), and 1198 (bronchial premalignant) cells.

To facilitate future translation into clinical trials, and because the absorption of grape seed procyanidin is affected by molecular weight [16, 17], we selected an inexpensive GSE reparation (leucoselect phytosome), standardized to smaller size grape seed oligomeric procyanidins (OPC) and complexed with soy phospholipids into phytosomes to improve bioavailability, for our *in vivo* preclinical efficacy study. In a previous clinical study, Leucoselect phytosome had been shown to improve the total antioxidant capacity of plasma

and reduce LDL susceptibility to oxidative stress in heavy smokers [18]. Oral gavage of leucoselect phytosome to athymic nude mice bearing A549 NSCLC xenografts significantly down-regulated the miR-17–92 cluster host gene (MIR17HG), miR-19a and miR-19b expressions, increased PTEN, IGF-2R and decreased phosphorylated AKT (P-AKT) protein levels in xenograft tumors, and markedly inhibited tumor growth.

To ascertain the bioavailability of leucoselect phytosome, procyanidin B1 in plasma samples obtained 60–90 minutes after oral gavage was measured as a marker of bioavailability. Interestingly, the estimated concentration of procyanidin B1 that was associated with 50% *in vitro* tumor cell growth inhibition (IC_{50}) (1.3 μg/ml) was much higher than the *in vivo* IC_{50} (0.032–0.13μg/ml) obtained in the athymic nude mouse tumor xenograft model. Our findings reveal novel anti-neoplastic mechanisms by GSE and support the further investigation of leucoselect phytosome as an anti-neoplastic and chemopreventive agent for lung cancer.

Aberrant expression of miRNA has been implicated in numerous disease states, including cancer. In the human genome, the miR-17–92 cluster encodes six miRNA species (miR-17, miR-18a, miR-19a, miR-20a, miR-19b-1, and miR-92–1), which are tightly grouped within an 800 base-pair region of chromosome 13, in the third intron of a ~7 kb primary transcript known as C13orf25 [19]. Expression of these miRNA promotes cell proliferation, suppresses apoptosis of cancer cells, and induces tumor angiogenesis. This is consistent with our findings that transfection of miR-19a and −19b mimics increased proliferation of lung neoplastic cells. By nature, miRNA appears to be enriched in blood and very stable in plasma, and are detectable with simple assays like qPCR. In a report that profiled miRNA in tumor, normal lung tissue, and plasma from subjects participating in lung cancer screening trials, various sets of miRNA signatures were found to be deregulated in plasma 1–2 years prior to and at the time of lung cancer diagnosis, including those in the miR-17–92 cluster [15]. Our findings therefore suggest the potential utility of miR-19a/b as SEBM for therapeutic monitoring of promising antineoplastic agents, including GSE.

The *PTEN* gene is mutated or inactivated in a large number of cancers at high frequency, including in NSCLC, resulting in reduced expression [20]. It specifically catalyzes the dephosphorylation of PIP_3 to PIP_2. This dephosphorylation is believed to inhibit the procarcinogenic phosphatidylinositol-3 kinase (PI3K)/AKT signaling pathway, as PIP_3 recruits AKT to the plasma membrane, enabling the activation of AKT by PDk1 via phosphorylation. The PI3 kinase/AKT signaling pathways are responsible for promoting cellular proliferation and resistance to apoptosis [21, 22]. As such, PTEN has been proposed as a candidate for targeted chemotherapy. Abrogation of PTEN function in malignant cells may occur through multiple mechanisms, from transcriptional to posttranslational modifications. Previous studies have shown that neither A549 nor H1299 cells harbor PTEN mutations, and the reduction of PTEN in H1299 cells is primarily due to promoter methylation [23, 24]. Therefore, the effects of GSE on PTEN in our model systems likely are not influenced by PTEN mutational status.

The insulin-like growth factor (IGF) pathway is involved in the normal control of fetal development, tissue growth, and metabolism. Deregulation of IGF signaling has been

described in several cancer types, including both small cell and non-small cell lung cancer [25]. Two distinct ligands IGF-1 and IGF-2 plus insulin, and two receptors, IGF receptor-1 (IGF-1R) and the insulin receptor, mediate the actions of this pathway. Downstream signaling is primarily through the PI3K/AKT pathway and the mitogen-activated protein kinase pathway, resulting in increased cell proliferation and apoptosis inhibition. IGF-2R plays a critical role in regulating the bioavailability of extracellular proteolytic enzyme and growth factors [26]. It clears IGF-2 from the cell surface to attenuate signaling, and has been shown to function as a tumor suppressor in a variety of cancer, including lung cancer [27–29]. Previous study in IGF-2-overexpressing rhabdomyosarcomas cells has shown that AKT phosphorylation on Ser473 may be the key target residue for PTEN to modulate the effects of IGF-2 on activating the PI3K/AKT pathways [28]. Collectively, our findings further support the notion that GSE may exert its antineoplastic effect through modulation of the IGF and PTEN signaling pathways (Fig 6).

Notably, a much lower concentration of GSE is required to bring about the same degree of antineoplastic effects in 1198 bronchial premalignant cells than A549 and H1299 cells. Whereas the precise mechanisms accounting for this variation in responsiveness to GSE are unclear and may be cell type specific, a plausible explanation is that precancerous cells are in general, more susceptible to anti-neoplastic agents, including GSE, than cancer cells, as they have not yet acquired all the molecular “machineries” that confer the malignant phenotype and resistance to antineoplastic agents. Whether or not the varying degree of miR-19a/b down-regulations observed in different cell lines is primarily responsible for the variable IC_{50} is also unclear, as regulation of miRNA is believed to be cell type, tissue, and even disease specific. Nonetheless, the substantially lower IC_{50} in 1198 cells further support the potential utility of GSE for lung cancer chemoprevention. In view of the heterogeneity of lung tumor biology, it is conceivable that GSE may exert differential, peri-transcriptional regulations of miR-19a/b expressions, leading to their variable reductions in different cell types.

All dosing regimen − 200, 300 and 400 mg/kg/day (containing GSE 56, 84, 112 mg/kg/day, respectively) for up to 8 weeks were well tolerated by nude mice. Plasma procyanidin B1 levels confirmed the absorption of oral administration of leucoselect phytosome, and the feasibility of this procyanidin as a marker of bioavailability in reference to the antineoplastic bioactivity *in vivo*, which was found to be markedly lower than the concentration required to achieve growth inhibition of NSCLC *in vitro*. This is the first study demonstrating the anti-neoplastic efficacy of leucoselect phytosome against lung cancer *in vivo*, thereby setting the stage for translation into clinical trials.

Lung cancer is the leading cause of cancer death in the world. Despite advancements in anticancer treatment, the 5-year survival for lung cancer remains dismal [30–32]. The lack of effective therapy provides the impetus to search for alternative, safe and efficacious agents for lung cancer chemoprevention, to impede the driving force of cancerization, and prevent lung cancer development in at-risk individuals [33]. In this study, we demonstrate novel GSE mediated anti-neoplastic mechanisms involving modulations of oncomirs and the efficacy of leucoselect phytosome against lung cancer; modulation of these mechanisms may also be

useful as SEBM in future clinical trials. Our findings provide important rationales to further investigate the potential of GSE for lung cancer treatment and chemoprevention.

Acknowledgement

We wish to thank J. Loewenheim, B. Wang, for their excellent technical assistance, S. Baca, A. Wagner and K. O'hair for animal care and training. Leucoselect phytosome was generously provided by Indena. This work is supported by grants from VA Merit Review (JTM, BX002258) and National Cancer Institute (JTM, R21CA173211).

REFERENCES

[1]. Cavaliere C, Foglia P, Gubbiotti R, Sacchetti P, Samperi R, Laganà A. Rapid-resolution liquid chromatography/mass spectrometry for determination and quantitation of polyphenols in grape berries. Rapid Commun Mass Spectrom 2008;22:3089–99. [PubMed: 18819110]

[2]. Shi J, Yu J, Pohorly JE, Kakuda Y. Polyphenolics in grape seeds-biochemistry and functionality. J Med Food 2003;6:291–9. [PubMed: 14977436]

[3]. Grape seed extract, herb at a glance. NCCAM. http://nccam.nih.gov/health/grapeseed/ataglance.htm

[4]. Dinicola S, Cucina A, Pasqualato A, D'Anselmi F, Proietti S, Lisi E, Pasqua G, Antonacci D, Bizzarri M. Antiproliferative and Apoptotic Effects Triggered by Grape Seed Extract (GSE) versus Epigallocatechin and Procyanidins on Colon Cancer Cell Lines. Int J Mol Sci 2012;13:651–64. [PubMed: 22312277]

[5]. Shrotriya S, Deep G, Gu M, Kaur M, Jain AK, Inturi S, Agarwal R, Agarwal C. Generation of reactive oxygen species by grape seed extract causes irreparable DNA damage leading to G2/M arrest and apoptosis selectively in head and neck squamous cell carcinoma cells. Carcinogenesis 2012;33:848–58 [PubMed: 22266465]

[6]. Akhtar S, Meeran SM, Katiyar N, Katiyar SK. Grape seed proanthocyanidins inhibit the growth of human non-small cell lung cancer xenografts by targeting insulin-like growth factor binding protein-3, tumor cell proliferation, and angiogenic factors. Clin Cancer Res 2009;15:821–31. [PubMed: 19188152]

[7]. Sharma SD, Meeran SM, Katiyar SK. Proanthocyanidins inhibit in vitro and in vivo growth of human non-small cell lung cancer cells by inhibiting the prostaglandin E(2) and prostaglandin E(2) receptors. Mol Cancer Ther 2010;9:569–80. [PubMed: 20145019]

[8]. Filipowicz W, Bhattacharyya SN, Sonenberg N. Mechanisms of post-transcriptional regulation by microRNAs: are the answers in sight? Nat Rev Genet 2008;9:102–14 [PubMed: 18197166]

[9]. Hammond SM, RNAi, microRNAs, and human disease. Cancer Chemother Pharmacol 2006;58:Suppl 1:s63–8. [PubMed: 17093929]

[10]. Mitchell PS, Parkin RK, Kroh EM, Fritz BR, Wyman SK, Pogosova-Agadjanyan EL, Peterson A, Noteboom J, O'Briant KC, Allen A, Lin DW, Urban N, Drescher CW, Knudsen BS, Stirewalt DL, Gentleman R, Vessella RL, Nelson PS, Martin DB, Tewari M.Circulating microRNAs as stable blood-based markers for cancer detection. Proc Natl Acad Sci U S A 2008;105:10513–8. [PubMed: 18663219]

[11]. Boeri M, Verri C, Conte D, Roz L, Modena P, Facchinetti F, Calabrò E, Croce CM, Pastorino U, Sozzi G. MicroRNA signatures in tissues and plasma predict development and prognosis of computed tomography detected lung cancer. Proc Natl Acad Sci U S A 2011;108:3713–8. [PubMed: 21300873]

[12]. Klein-Szanto AJ, Iizasa T, Momiki S, Garcia-Palazzo I, Caamano J, Metcalf R, Welsh J, Harris CC. A tobacco-specific N-nitrosamine or cigarette smoke condensate causes neoplastic transformation of xenotransplanted human bronchial epithelial cells. Proc Natl Acad Sci U S A. 1992;89:6693–7. [PubMed: 1323115]

[13]. Tomayko MM, Reynolds CP. Determination of subcutaneous tumor size in athymic (nude) mice. Cancer Chemother Pharmacol. 1989;24:148–54. [PubMed: 2544306]

[14]. Mao JT, Nie WX, Tsu IH, Jin YS, Rao JY, Lu QY, Zhang ZF, Go VL, Serio KJ. White tea extract induces apoptosis in non-small cell lung cancer cells: The role of peroxisome proliferator-activated receptor-{gamma} and 15-lipoxygenases. Cancer Prev Res. 2010;3:1132–40.

[15]. Olive V, Bennett MJ, Walker JC, Ma C, Jiang I, Cordon-Cardo C, Li QJ, Lowe SW, Hannon GJ, He L. miR-19 is a key oncogenic component of mir-17–92. Genes Dev 2009;15:23:2839–49.

[16]. Deprez S, Mila I, Huneau JF, Tome D, Scalbert A. Transport of proanthocyanidin dimer, trimer, and polymer across monolayers of human intestinal epithelial caco-2 cells. Antioxid Redox. Signal 2001;3:957–67. [PubMed: 11813991]

[17]. Scalbert A, Williamson G, Dietary intake and bioavailability of polyphenols. J. Nutr 2000;130:2073S–2085S. [PubMed: 10917926]

[18]. Vigna GB, Costantini F, Aldini G, Carini M, Catapano A, Schena F, Tangerini A, Zanca R, Bombardelli E, Morazzoni P, Mezzetti A, Fellin R, Maffei Facino R. Effect of a standardized grape seed extract on low-density lipoprotein susceptibility to oxidation in heavy smokers. Metabolism 2003;52:1250–57. [PubMed: 14564675]

[19]. Mendell JT. MiRiad roles for the miR-17–92 cluster in development and disease. Cell 2008;133: 22.

[20]. Hollander MC, Blumenthal GM, Dennis PA PTEN loss in the continuum of common cancers, rare syndromes and mouse models. Nat. Rev. Cancer 2011;11:289–301. [PubMed: 21430697]

[21]. Stambolic V, Suzuki A, de la Pompa JL, Brothers GM, Mirtsos C, Sasaki T, Ruland J, Penninger JM, Siderovski DP, Mak TW. Negative regulation of PKB/Akt-dependent cell survival by the tumor suppressor PTEN. Cell 1998;95:29–39. [PubMed: 9778245]

[22]. Wu X, Senechal K, Neshat MS, et al. The PTEN/MMAC1 tumor suppressor phosphatase functions as a negative regulator of the phosphoinositide 3-kinase/Akt pathway. Proc Natl Acad Sci USA 1998;95:15587–91. [PubMed: 9861013]

[23]. Kohno T, Takahashi M, Manda R, Yokota J. Inactivation of the PTEN/MMAC1/TEP1 gene in human lung cancers. Genes Chromosomes Cancer 1998:22:152–6. [PubMed: 9598803]

[24]. Soria JC, Lee HY, Lee JI, et al. Lack of PTEN expression in non-small cell lung cancer could be related to promoter methylation. Clin Cancer Res 2002;5:1178–84.

[25]. Dziadziuszko R, Camidge DR, Hirsch FR. The insulin-like growth factor pathway in lung cancer. J Thorac Oncol 2008;3:815–8. [PubMed: 18670298]

[26]. Lee HY, Jung H, Jang IH, Suh PG, Ryu SH. Cdk5 phosphorylates PLD2 to mediate EGF-dependent insulin secretion. Cell Signal 2008;20:1787–94. [PubMed: 18625302]

[27]. Kreiling JL, Montgomery MA, Wheeler JR, Kopanic JL, Connelly CM, Zavorka ME, Allison JL, Macdonald RG. Dominant-negative effect of truncated mannose 6-phosphate/insulin-like growth factor II receptor species in cancer. FEBS J 2012;279:2695–713. [PubMed: 22681933]

[28]. Kong FM, Anscher MS, Washington MK, et al. M6P/IGF2R is mutated in squamous cell carcinoma of the lung. Oncogene 2000;19:1572–8. [PubMed: 10734317]

[29]. Wan X, Helman, Li. Levels of PTEN protein modulate akt phosphorylation on serine 473, but not on threonine 308, in IGF-II-overexpressing rhabdomyosarcomas cells. Oncogene 2003:22:8205–11. [PubMed: 14603261]

[30]. Burns DM. Tobacco smoking. In: Samet J, editor. In Epidemiology of Lung Cancer. New York: Marcel Dekker, Inc.; 1994. p. 15–9.

[31]. Fry WA, Menck HR, Winchester DP. The national cancer data base report on lung cancer. Cancer 1996;77:1947–55. [PubMed: 8646697]

[32]. American Cancer Society. Cancer Facts and Figures 2008. Atlanta: American Cancer Society; 2008.

[33]. Mao JT, Durvasula R. Lung Cancer Chemoprevention: Current Status and Future Direction. Curr Respir Care Rep 2012;1:9–20.

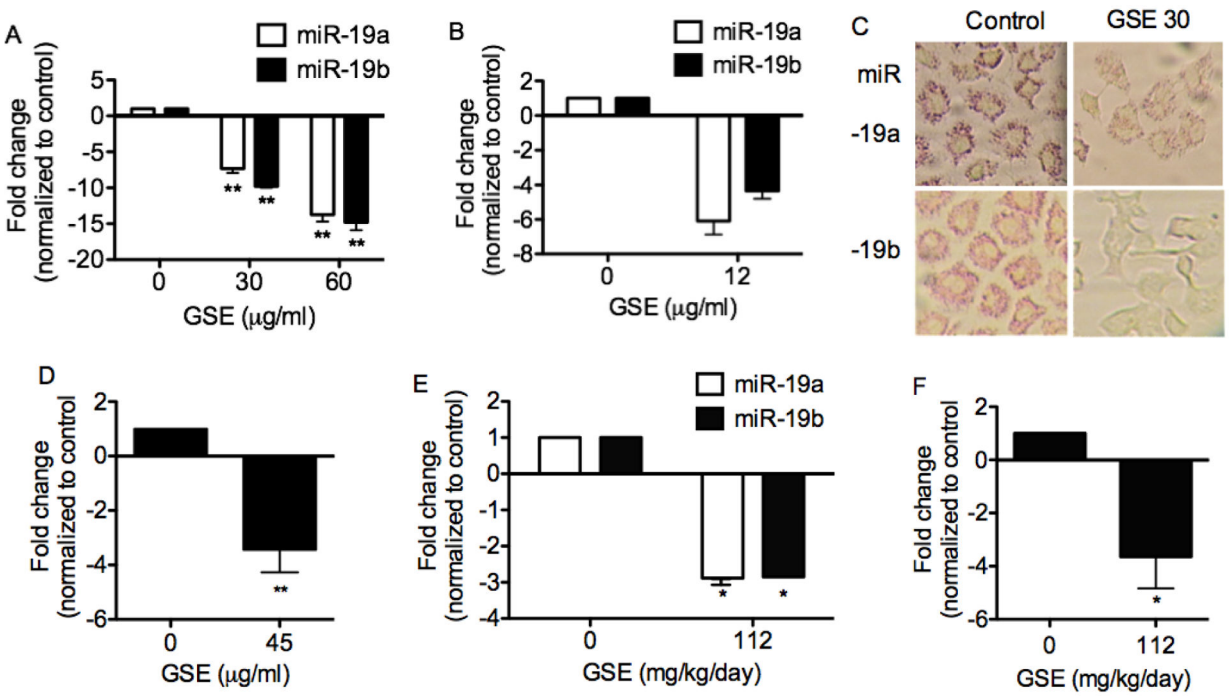

Fig. 1.

GSE significantly down-regulates oncomir miR-19a, and −19b expression in lung neoplastic cells. MiRNA specific qPCR demonstrate down-regulation of these miRNA in (A) A549 (n = 3) and (B) 1198 (n = 2) cells. Mir-19a and −19b ISH assays further confirm the down-regulation of these miRNA in A549 cells by GSE (30 μg/ml). (C) Representative photomicrograph of miR-19a and −19b specific ISH assay with fast red stain in conditioned A549 cells. Magnification: 400X. (D) GSE also significantly down-regulates the expression of miR-19a/b host gene, MIR17HG (n=3). In addition, 8 weeks of Leucoselect phytosomes (GSE:soy phosophlipids,112:400 mg/kg/day), administered to athymic nude mice bearing A549 NSCLC xenografts via gavage, significantly decreases expression of (E) miR-19a/b and (F) MIR17HG in the tumor xenografts (n = 5). Columns, mean; bars, SD. **, $P < 0.01$.

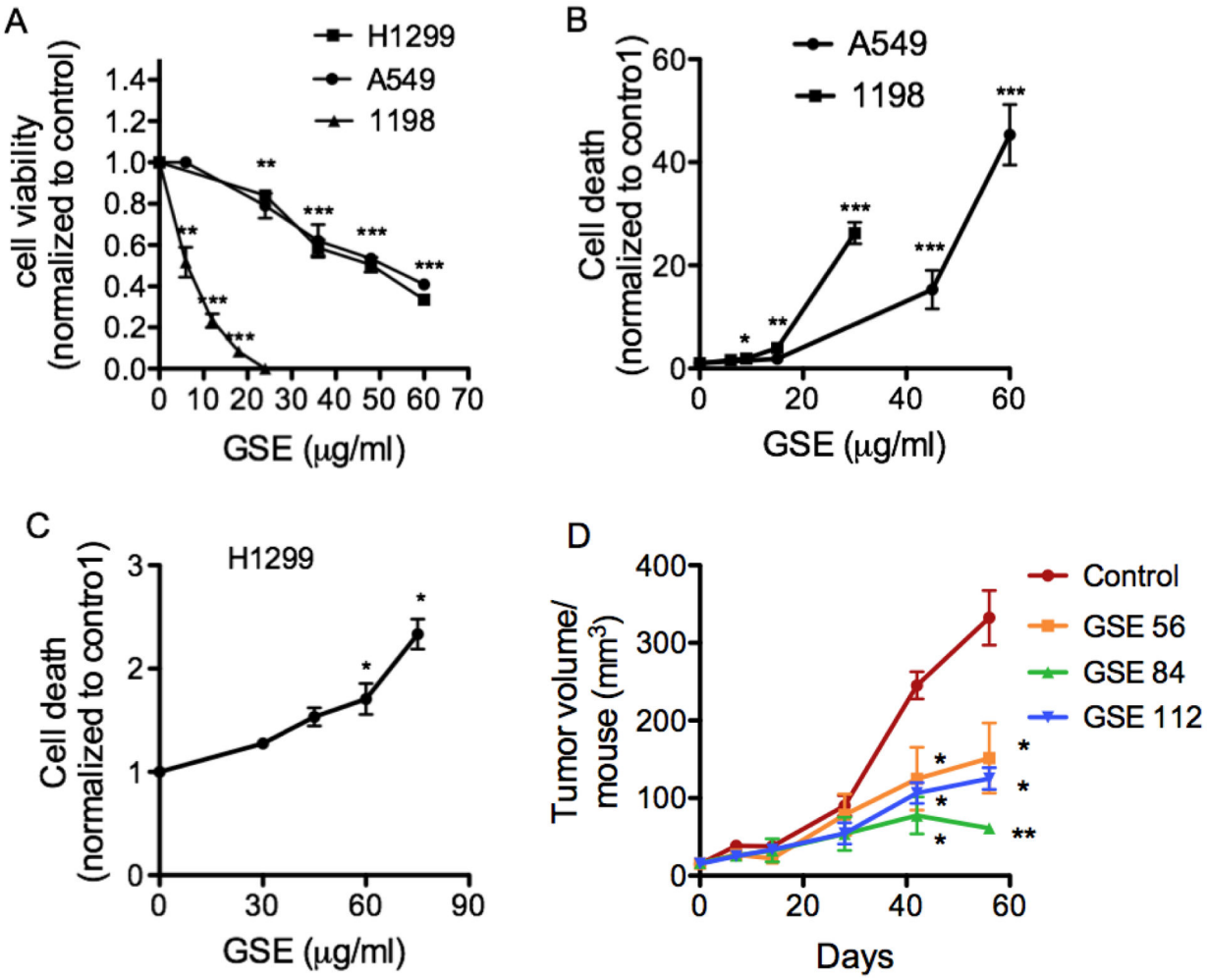

Fig. 2.

GSE dose-dependently induces anti-proliferative and apoptotic changes in lung neoplastic cells, following 24h of incubation. (A) Quantification of cell proliferation in conditioned A549, H1299 and 1198 cells by MTT assay. (B) Quantification of apoptosis in conditioned A549, 1198 and (C) H1299 cells by cell death detection ELISA, as measured by specific determination of mononucleosomes and oligonucleosomes in the cytoplasmic fraction of cell culture lysates; The mean ± SD absorbance values at 405 nm are reported. Control = 0 μg/ml GSE. (D) Oral administration of varying doses of leucoselect phytosomes (0, 200, 300, and 400 mg/kg/day, containing 0, 56, 84, 112 mg GSE/kg body weight/day, respectively) significantly inhibited A549 xenograft tumor growth (n = 9 per group). Columns, mean; bars, SD. *, $P < 0.05$. **, $P < 0.01$, ***, $P < 0.001$.

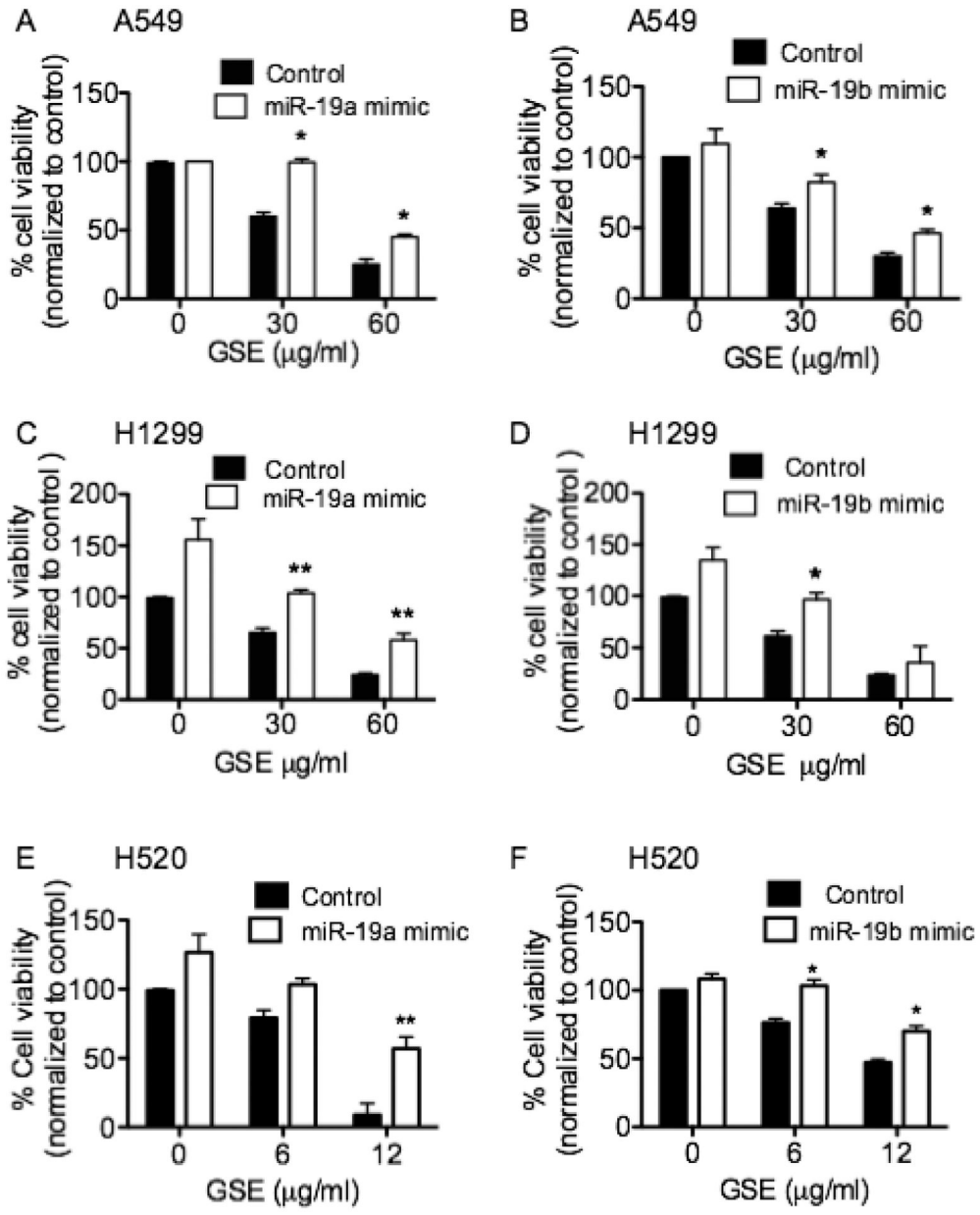

Fig. 3.

Transfections of miR-19a & −19b mimics significantly reverse the anti-proliferative effects of GSE in (A & B) A549, and (C & D) H1299, (E & F) H520 and 1198 cells (data not shown), as measured by MTT assays. Columns, mean; bars, SD (n = 3). *, $P < 0.05$. **, $P < 0.01$. Control represents cells treated with negative control (scrambled oligonucleotides).

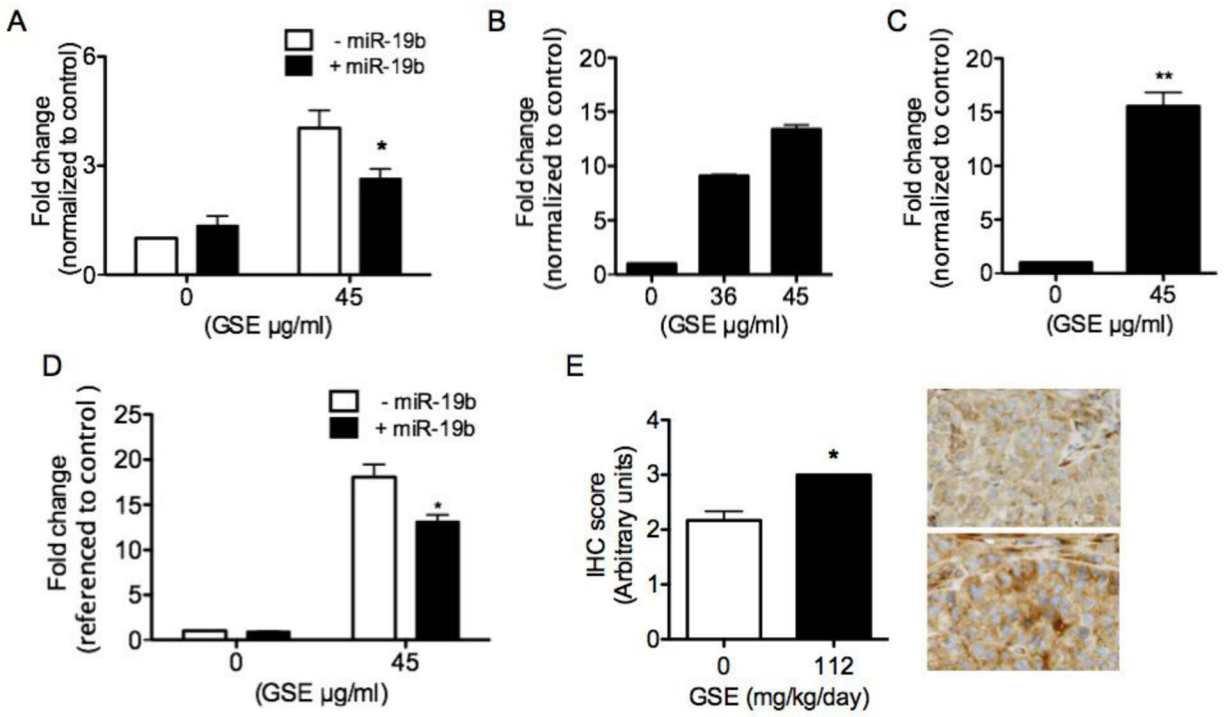

Fig. 4.

GSE significantly increases (A) *IGF2R* mRNA expression, (B) protein production (as measured in cell lysates, n = 2) and (C) secretion (as measured in culture supernatants) in A549 cells conditioned with GSE overnight (45 µg/ml, 16–18h incubation). (D) Transfection of A549 cells with miR-19b mimics significantly reverses GSE-induced up-regulation of *IGF2R mRNA* and protein production. IGF-2R levels are first referenced to total protein levels, the values are then normalized to control. The range of control IGF-2R levels is 754 to 802 pg/ml. (E) Oral gavage of nude mice with leucoselect phytosome (GSE=112 mg/kg/day) for 8 weeks also increases IGF-2R in A549 xenograft tumors. Representative photomicrographs of IGF-2R IHC in xenografft tumors: top, from mouse gavaged with water; bottom, from mouse gavaged with leucoselect phytosome; magnification − 400X. Columns, mean; bars, SD (n = 3). *, $P < 0.05$, **, $P < 0.01$).

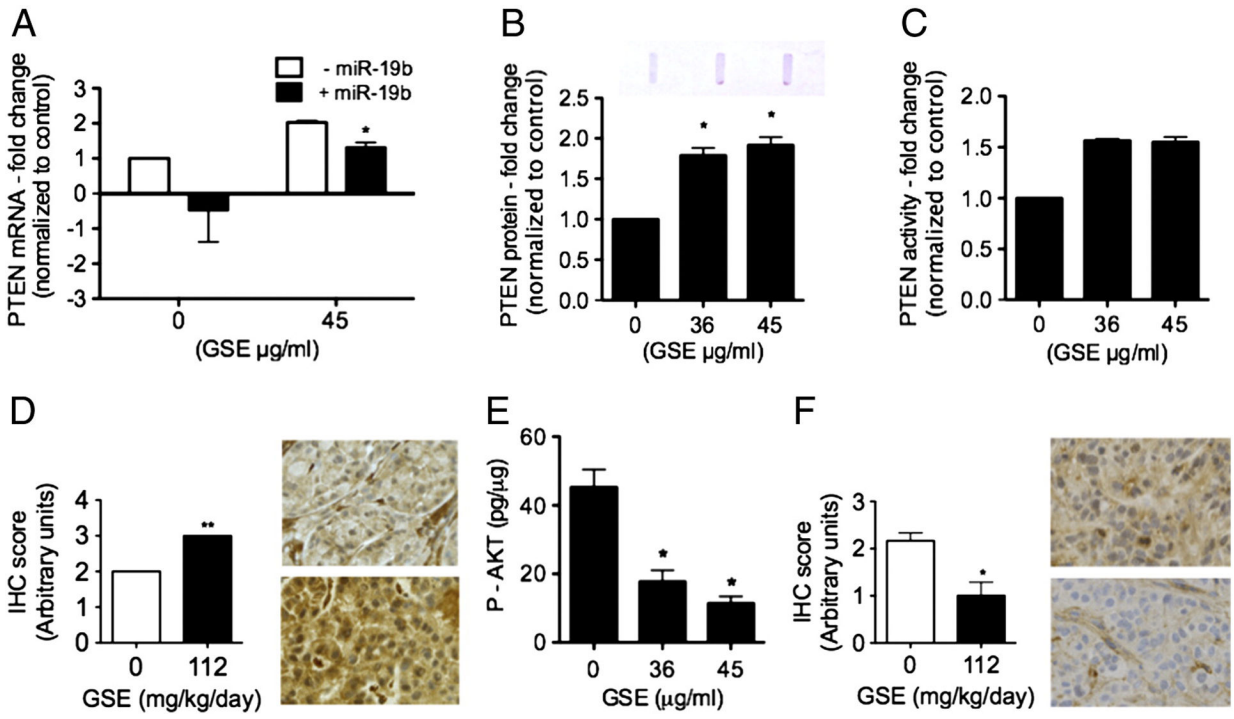

Fig. 5.

GSE increases (A) *PTEN* mRNA expression, and transfection of miR-19b mimics abrogated the GSE induced up-regulation of *PTEN*. GSE also increased (B) PTEN protein production in A549 cells (GSE 45 µg/ml, 16–18h incubation). PTEN levels in GSE-conditioned A549 cells were determined semi-quantitatively using immuno-slot blots with PTEN-specific mAb. Top: representative photograph of PTEN blot. Furthermore, GSE increased (C) PTEN activity in A549 cells, as measured by conversion of PIP_3 to PIP_2 (C, n = 2). (D) IHC scoring of PTEN in xenograft tumors further confirms its increase by leucoselect phytosome (GSE = 112 mg/kg/day, 8 weeks treatment) *in vivo*. Representative photomicrographs of PTEN IHC in xenograft tumors: top, from mouse gavaged with water; bottom, from mouse gavaged with leucoselect phytosome; magnification − 400X. Moreover, GSE significantly (E) decreased AKT phosphorylation on Ser473 in A549 cells (GSE 45 µg/ml, 16–18h incubation). P-AKT levels (pg/ml) were normalized to total protein (µg/ml) in conditioned cell lysates. (F) IHC scoring of p-AKT in xenograft tumors confirms the reduction of P-AKT by leucoselect phytosome (GSE = 112 mg/kg/day, 8 weeks treatment) *in vivo*. Representative photomicrographs of P-AKT IHC in xenografft tumors: top, from mouse gavaged with water; bottom, from mouse gavaged with leucoselect phytosome; magnification − 400X (F). Columns, mean; bars, SD (n = 3). *, $P < 0.05$.

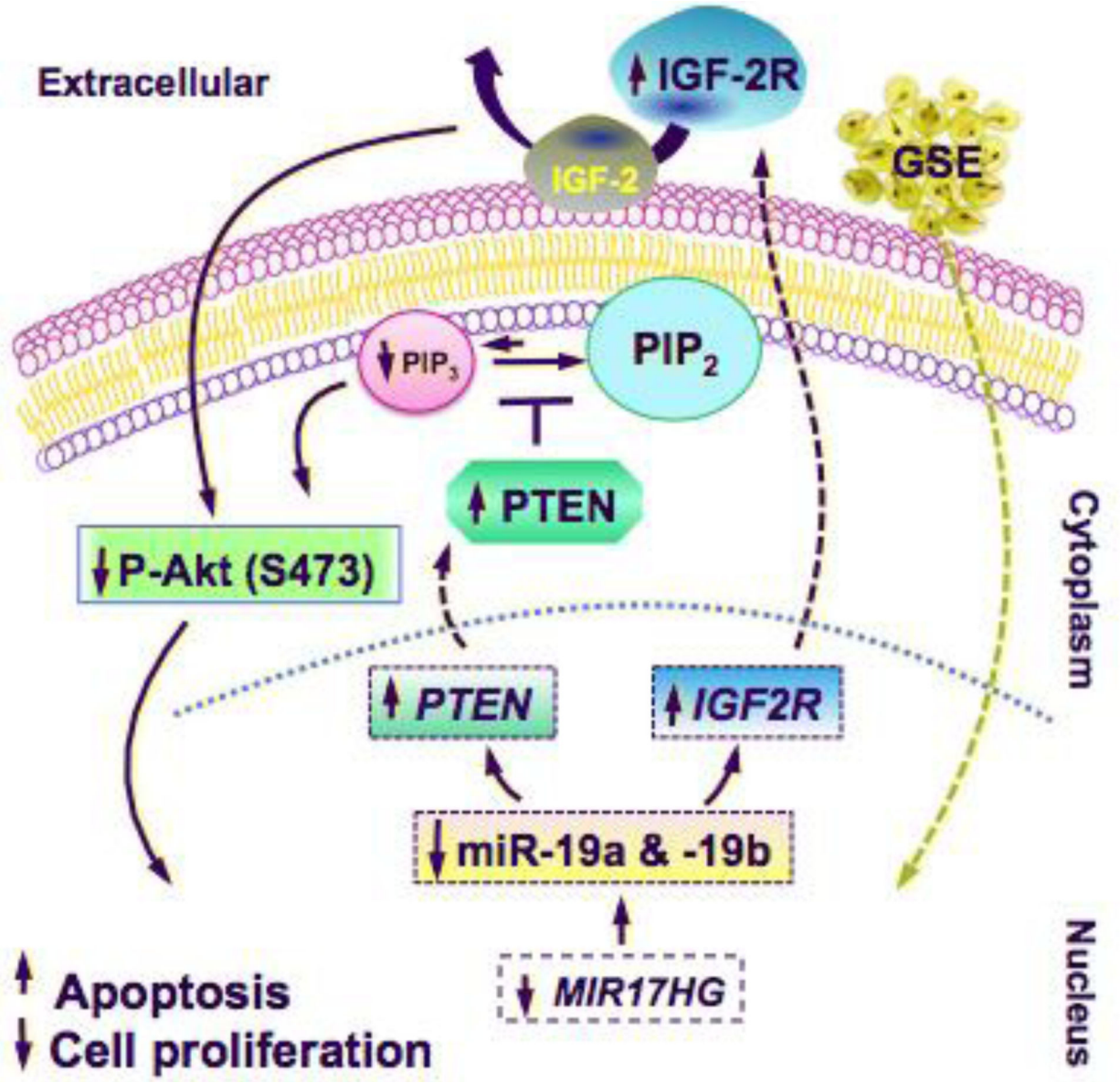

Fig. 6.

Schematic illustrations of the proposed anti-neoplastic mechanisms of GSE against lung cancer. GSE significantly down-regulated the expression of miR-19a/b and their host gene, *MIR17HG,* which in turn up-regulated the mRNA expression of tumor suppressor genes *IGF2R* and *PTEN,* their respective protein products, and decreased P-AKT. These mechanisms contributed to induction of apoptosis and inhibition of cell proliferation in lung neoplastic cells. Our findings indicate that the antineoplastic properties of GSE are mediated, in part, through modulations of oncomirs miR-19a and −19b.

Table 1.

Mouse plasma procyanidin B1 levels at week 2 and 8 of treatment

	Water	Leucoselect phytosome (400mg/kg)
Week 2	ND	32.4 ng/ml
Week 8	ND	130 ng/ml

ND = not detectable.